1 **Supporting Information**

2

3

4 Bimetallic nanozymes synergize to regulate the behavior of oxygen

5 intermediates and substrate HMF adsorption

6

7 Lei Shi[a], Qiang Li[c], Shuang Liu[a], Xinyang Liu[a], Shucheng Yang[a], Chunxia Chen[*a], Zhijun Li[*b], Song

8 Liu[*a]

9 [a] Chemical Engineering and Resource Utilization, Northeast Forestry University, Harbin 150040,

10 China.

11 [b] Key Laboratory of Functional Inorganic Materials Chemistry (Ministry of Education), School of

12 Chemistry and Materials Science, Heilongjiang University, Harbin 150080, P. R. China.

13 [c] Inner Mongolia Institute of Synthetic chemistry，Hohhot 010010, China.

Experimental Section

Materials and Chemicals

16 **Reagents and Materials.** Cobalt nitrate hexahydrate ($Co(NO_3)_2 \cdot 6H_2O$)**,** Nickel nitrate

17 hexahydrate ($Ni(NO3)_2 \cdot 6H_2O$), hydrochloric acid (HCl), potassium hydroxide (KOH),

18 and ethanol were bought from Tianjin Kermel Chemical Reagent Company. Sodium

19 hypophosphite ($NaH_2PO_2 \cdot H_2O$), Potassium hydroxide (KOH), sodium hydroxide

20 (NaOH), sodium carbonate (Na_2CO_3), dimethyl sulfoxide (DMSO) and 3,3`,5,5`-

21 Tetramethylbenzidine (TMB) were purchased from Macklin Co., Ltd. (Shanghai,

22 China). 5-hydroxymethylfurfural (HMF), 2,5-furandicarboxylic acid (FDCA), 5-

23 hydroxymethyl-2-furancarboxylic acid (HMFCA), and 5-formyl-2-furancarboxylic

24 acid (FFCA) were purchased from Alfa-Aesar. 2,5-diformylfuran (DFF) was purchased

25 from Tokyo Chemical Industry Co., Ltd. 5 wt% Nafion solution was purchased from

26 the Sigma Co., Ltd. Nickel foam was purchased from Suzhou Sinero Technology Co.,

27 Ltd. Nafion 117 membrane was purchased from Wuhan GaossUnion technology Co.,

28 Ltd.

Preparation of Mimic Enzymes.

30 As shown in Figure 1a, 40 mL of 1 M salt solution was slowly added under stirring into

31 a reactor containing 200 mL of water. The reaction pH was maintained at a constant

32 value of 10 by the simultaneous addition of an alkaline solution (2 M NaOH, 0.5 M

33 Na_2CO_3). After 24 h, the reaction was stopped, and the slurry was centrifuged, washed

34 three times with deionized water, and dried at room temperature. Then, a part of the

35 coprecipitation medium and clean nickel foam was transferred into a 40 mL capacity

36 Teflon-lined stainless steel autoclave and heated at 120 ℃ under autogenous pressure

37 for 24 h. After the hydrothermal treatment, the autoclave was allowed to cool down to

38 room temperature, and the resulting precipitate was recovered by centrifugation. The

39 loaded nickel foam was washed several times through water and ethanol and then dried

40 at room temperature.

Synthesis of CoNiP, CoP, and NiP

42 Briefly, NaH_2PO_2 and Pre-CoNi were placed upstream and downstream in a corundum

tube of the tube furnace, respectively. Then, CoNiP was obtained by calcining the Pre-CoNi at 350 °C for 2 hours (rising temperature rate =2 °C min^{-1}) under a nitrogen flow. Meanwhile, CoP and NiP were prepared via a similar phosphorization method to CoNiP. Only the corresponding precursors were changed.

Mimic Enzyme Activity Assay. The oxidase-like activity of samples was evaluated by direct catalytic oxidation of TMB. In the typical procedure, 400 µL of TMB solution (5 mM DMSO) was added into 3mL of acetate buffer (1 M, pH=4.5), then injecting 50 µL of catalyst aqueous solution (1 mg/mL). Subsequently, the color reaction was monitored by determining the absorbance with a UV-vis spectrometer.

Characterization.

Scanning electron microscopy (SEM) and transmission electron microscopy (TEM) images were collected by using a Zeiss Gemini 300 microscope and a JEM 2100 F microscope, respectively. Elemental mappings were detected through energy-dispersive X-ray (EDX) spectroscopy. Powder X-ray diffraction (XRD) patterns were recorded on a Thermo Ultima IV X-ray diffractometer. X-ray photoelectron spectroscopy (XPS) was analyzed via Thermo Scientific Escalab 250Xi. Electron paramagnetic resonance

(EPR) spectra were recorded on a Bruker EMXplus-6/1 spectrometer. An electrochemical workstation (CHI660E) was employed to analyze electrochemical impedance spectroscopy (EIS), cyclic voltammograms, and Tafel polarization curves in the 1 M KOH, wherein Ag/AgCl electrode and platinum electrodes acted as reference electrode and counter electrode, respectively.

The steady-state kinetic analyses

The kinetic analysis was carried out according to the Michaelis−Menten equation as follows:

$$\frac{1}{V} = \left(\frac{Km}{Vmax}\right) * \left(\frac{1}{[S]}\right) + \frac{1}{Vmax}$$

where Km is the Michaelis constant, *Vmax* is the maximum reaction velocity, and [S] is the TMB concentration.

Electrochemical Measurements

We conducted electrochemical measurements on a CHI 660E electrochemical workstation. Electrochemical data were collected at room temperature in an H-type cell (50 mL), in which the two chambers were separated by a Nafion 117 proton exchange membrane. The electrochemical tests were carried out with the three-electrode configuration, the as-synthesized catalyst on Ni foam (≈1.0 × 1.0 cm) was directly used as the working electrode, a silver/silver chloride (Ag/AgCl) and a platinum sheet (area: 2 cm^2) were used as the reference electrode and counter electrode, respectively. 1.0 M KOH (pH=13.8) with or without different concentrations of HMF were used as the electrolytes. Linear sweep voltammetry (LSV) was collected until the test results were kept stable at a scan rate of 5 mV s^{-1}. All potentials in this study were referred to the reversible hydrogen electrode (RHE) according to the following equation:

$E_{RHE} = E_{Ag/AgCl} + 0.197\ V + 0.0592·pH$ (1)

Estimation of the electrochemical surface area: The electrochemical surface area

1 (ECSA) of the electrocatalyst was estimated from the electrochemical double-layer
2 capacitance (C_{dl}), which was investigated via cyclic voltammetry (CV) cycles. The CV
3 was performed in 1.0 M KOH containing 5 mM HMF at various scan rates of 20, 40,
4 60, 80, and 100 mV s^{-1} in a non-faradaic potential window. Electrochemical impedance
5 spectroscopy (EIS) tests were measured over a frequency range from 10^{-2} to 10^{6} Hz
6 with an AC amplitude of 10 mV. The tests were carried out with the typical three-
7 electrode configuration at 1.4 V *vs*. RHE.

8 **Products analysis**

9   The HMF, intermediates (HMFCA, FFCA, HMF, and DFF), and oxidation
10 product (FDCA) were analyzed by high-performance liquid chromatography (HPLC,
11 Agilent 1290 Infinity II) with an ultraviolet (UV)–visible detector (wavelength: 265
12 nm) and a Shim-pack GWS C18 (5 μm, 4.6 ×150 mm) column. The used electrolyte
13 was 1 M KOH solution containing 40 mL 5 mM HMF. The mobile phase was 75%
14 ammonium formate together with 25% methanol. The flow rate was 0.2 mL min^{-1}.
15 Before applying a constant potential, 50 μL analyte was mixed with 950 μL water. This
16 mixture with a volume of 3 μL was then injected into the HPLC. The column
17 temperature was maintained at 35 °C, and each separation lasted for 25 min.
18 The conversion of HMF and the selectivity, faradaic efficiency (FE), and yield rate of
19 FDCA were calculated according to Equations (2-4), respectively.

20 HMF conversion (%) = [n(HMF consumed) / n(HMF initial)] × 100   (2)
21 Product yield (%) = [n(product) / n(HMF initial)] × 100   (3)
22 Faradaic efficiency (%) = [n(FDCA formed) / (Q / (6 × F))] × 100   (4)
23 Where Q is the total transferred charge, F represents the Faraday constant (96485 C
24 mol^{-1}), and n is the mole number of reactant.

25 **In Situ Raman Spectroscopy**

26   *In situ* Raman experiments were carried out on a Cu belt. The electrolytic cell for in
27 situ Raman Spectrum comprises a Teflon shell, Cu belt, Pt wire, and Ag/AgCl
28 electrodes. All the electrochemical tests were carried out using the three-electrode
29 configuration connected to an electrochemical workstation (CHI-660E). The counter
30 electrode was a platinum wire for HER. The electrolyte is 1 M KOH with or without
31 HMF for the HMF electrooxidation and OER testing.

32 **Density functional theory (DFT) Calculation**

33   The generalized gradient approximation (GGA)[1] with the Perdew–Burke–
34 Ernzerhof exchange-correlation functional was employed to carry out the density
35 functional theory (DFT) computations of the researched systems within the frame of
36 Vienna ab initio simulation package (VASP).[2, 3] The DFT-D3 is used to describe van
37 der Waals forces   (vdW)[4, 5] correction was included to correct the dispersion
38 interactions. The projector-augmented plane wave (PAW)[6, 7] was used for the
39 description of the electronic interactions, and the kinetic energy cutoff was set as 500
40 V for the plane wave expansion. We build a 2 × 2-supercell of the CoNiP one molecule

1 thick, the 20 Å vacuum layer was constructed to avoid interactions between the layers

2 (Figure S11). The full relaxation of the geometric structures was adopted $7\times7\times1$

3 Monkhorst-Pack grid k-points and their density of states (DOSs) was computed. The

4 convergence threshold is set as 10^{-5} eV in energy and 0.02 eV Å^{-1} in force.

5   The reaction-free energy (ΔG) calculations were performed using the Computational

6 Hydrogen Electrode (CHE) model. In this method, the chemical potential of ($H^+ + e^-$) is

7 equal to half the chemical potential of H_2. The ΔG for each step is given by the equation:

8

9 $$\Delta G = \Delta E - T\Delta S + \text{ZPE} - |e|U.$$

10   where ΔE, ZPE, and ΔS correspond to the change in the total energy directly obtained

11 from DFT calculation and the differences of zero-point energy and entropy before and

12 after adsorption, respectively. T is set to 298.15K.

13   The adsorption energy of H_2O on the doped surface was calculated using the

14 following formula:

15 $$\Delta E_{ads} = E_{*H2O} - E_* - E_{H2O}$$

16 where E_{*H2O} is the total energy of the adsorbed H_2O on the catalyst, E_* is the energy of

17 the catalyst itself, and E_{H2O} is the total energy of H_2O.
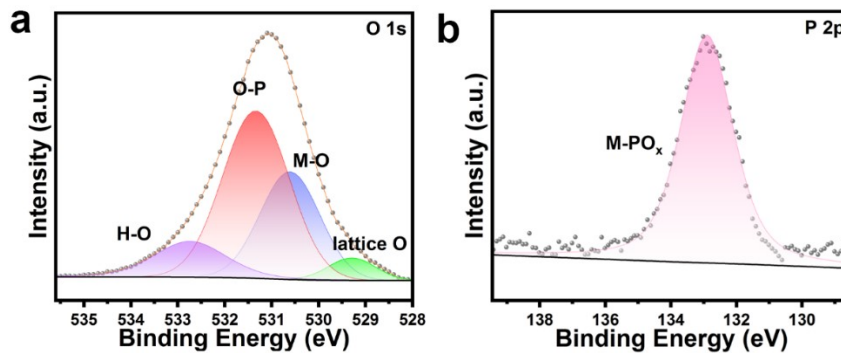
18

19 Fig. S1 XPS spectra of the CoNiP: (a) O 1s, (b) P 2p.
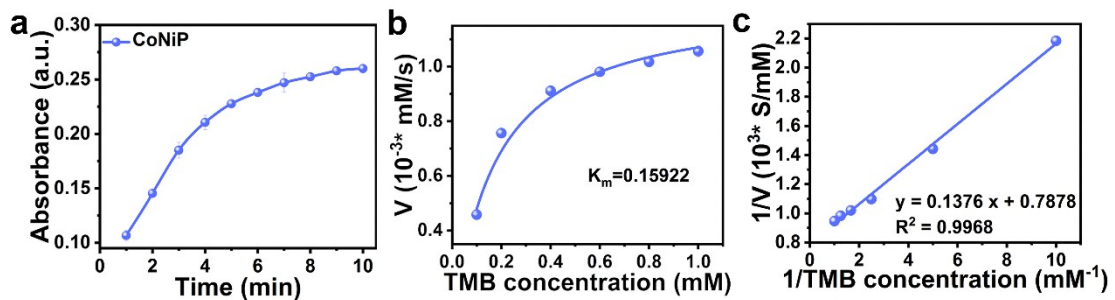
20

1 Fig. S2 The steady-state kinetic analysis of CoNiP enzyme-like catalysts after stored
2 at room temperature for 30 days.
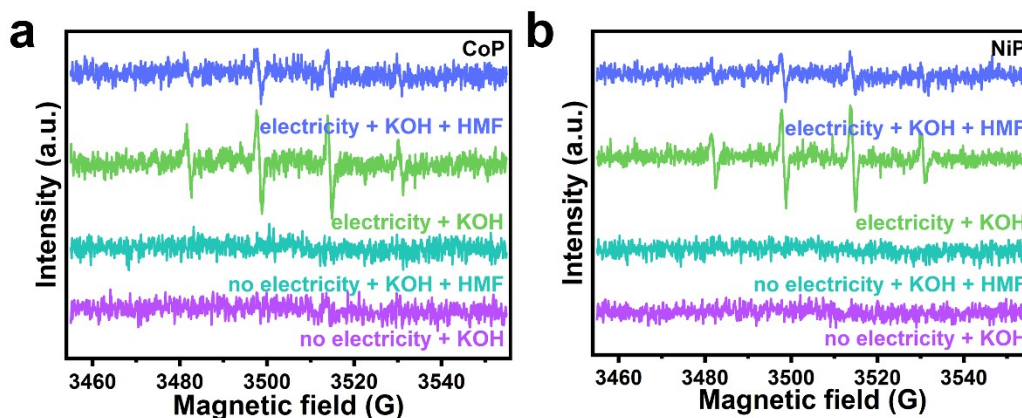
3
4 Fig. S3 EPR spectra of CoNiP over different reaction conditions.
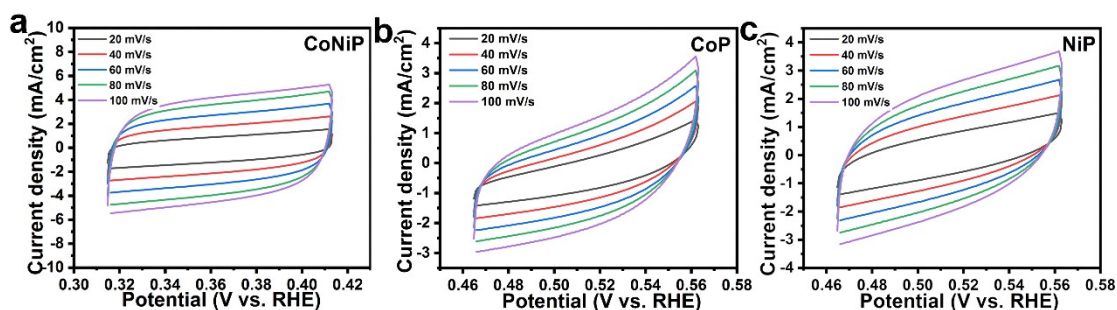
5
6 Fig. S4 Cyclic voltammograms of (a) CoNiP, (b) CoP, (c) NiP.
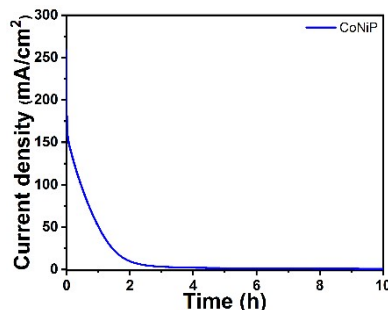
7
8 Fig. S5 Corresponding current changes over time of the chronoamperometry test of
9 CoNiP at 1.4 V in 1.0 M KOH with 5 mM HMF.
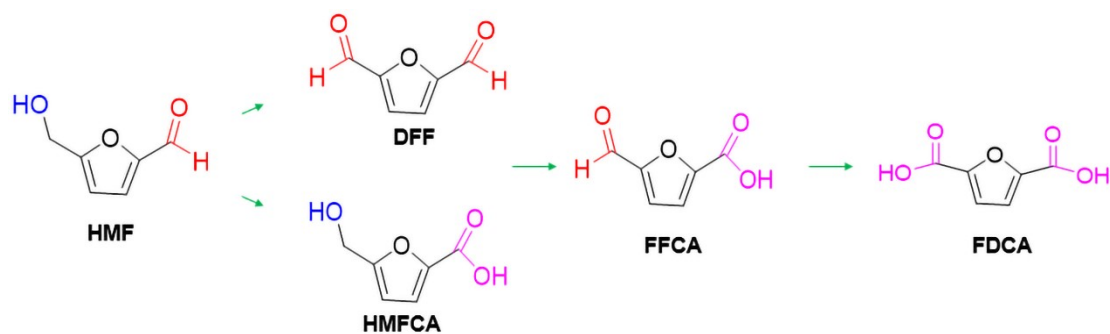
10
11 Fig. S6 Two pathways of HMF oxidation reactions.
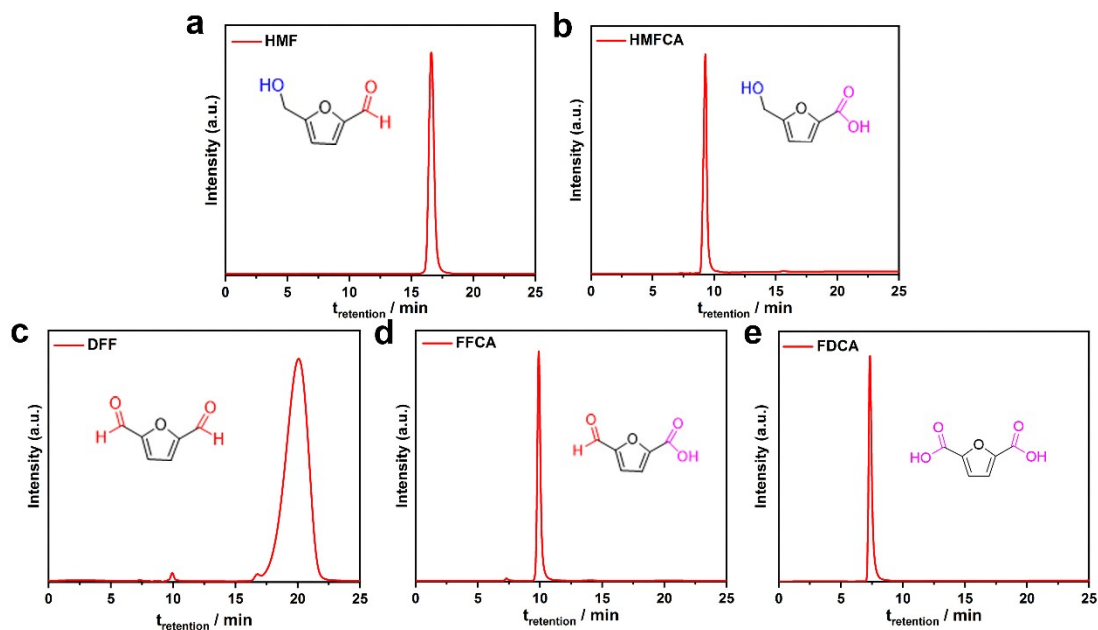
1

2 Fig. S7 HPLC traces of the HMF and intermediates (HMFCA, DFF, and FFCA) and

3 final oxidation product FDCA. The mobile phase was 75% ammonium formate together

4 with 25% methanol. The flow rate was 0.2 mL min^{-1}. The column temperature was

5 maintained at 35 °C, and each separation lasted for 25 min.
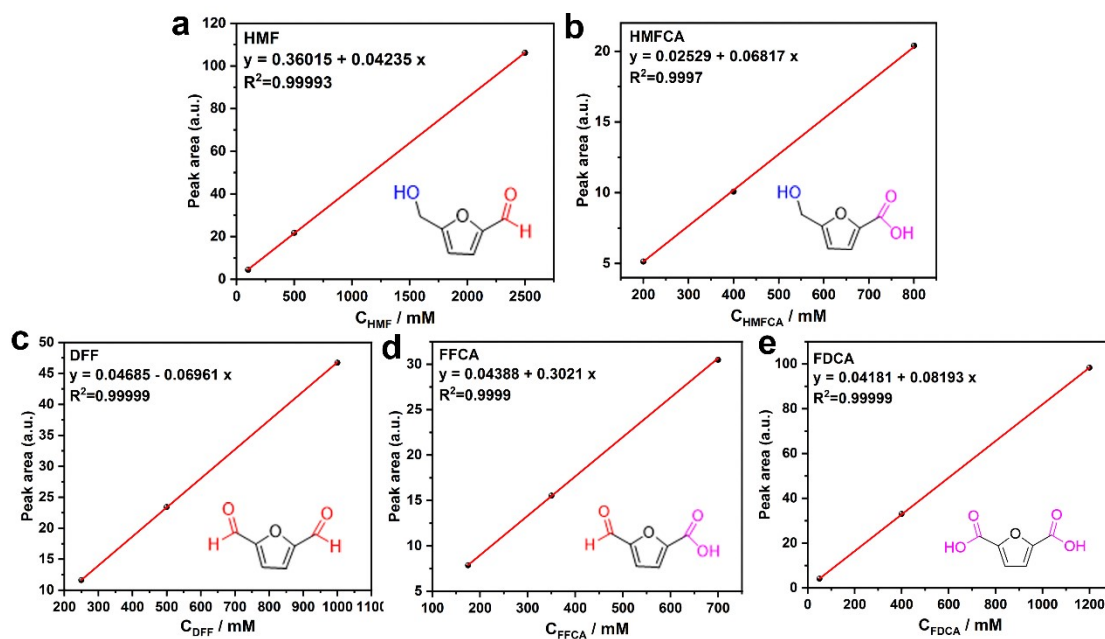
6

7 Fig. S8 HPLC standard curves of (a) HMF, (b) DFF, (c) HMFCA, (d) FFCA, (e)

8 FDCA.
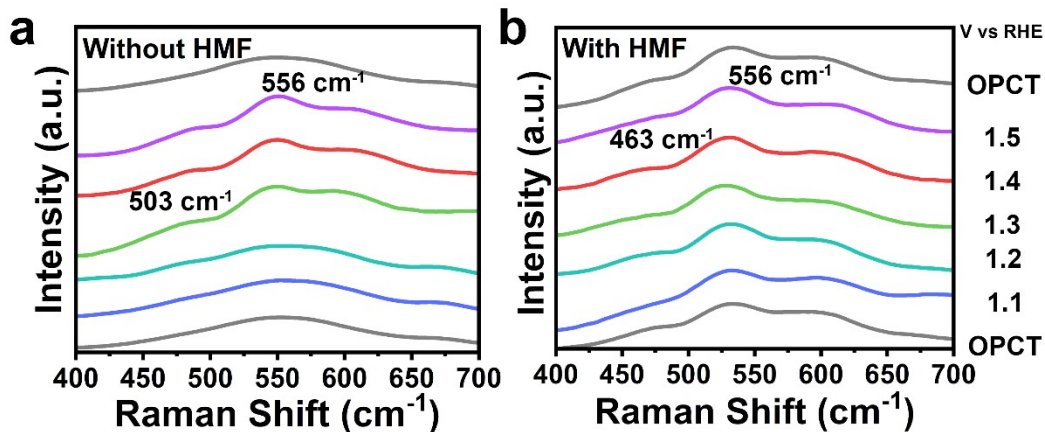
Fig. S9 *In situ* Raman spectra of CoNiP in 1 M KOH (a) without and (b) with 10 mM HMF in different potentials.
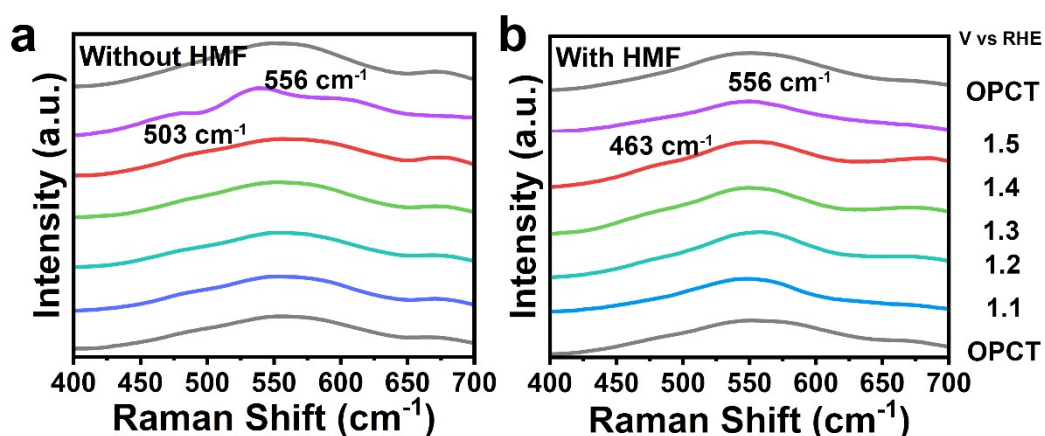
Fig. S10 *In situ* Raman spectra of CoP in 1 M KOH (a) without and (b) with 10 mM HMF in different potentials.
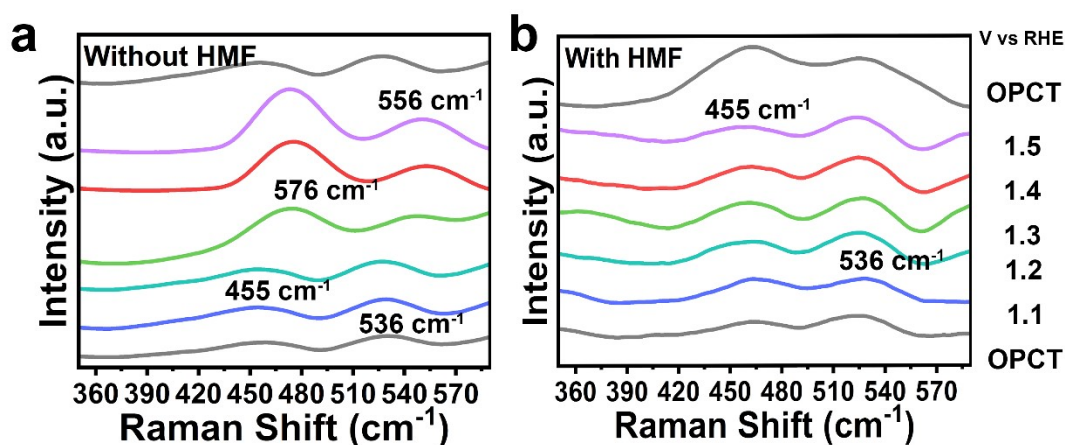
Fig. S11 *In situ* Raman spectra of NiP in 1 M KOH (a) without and (b) with 10 mM HMF in different potentials.
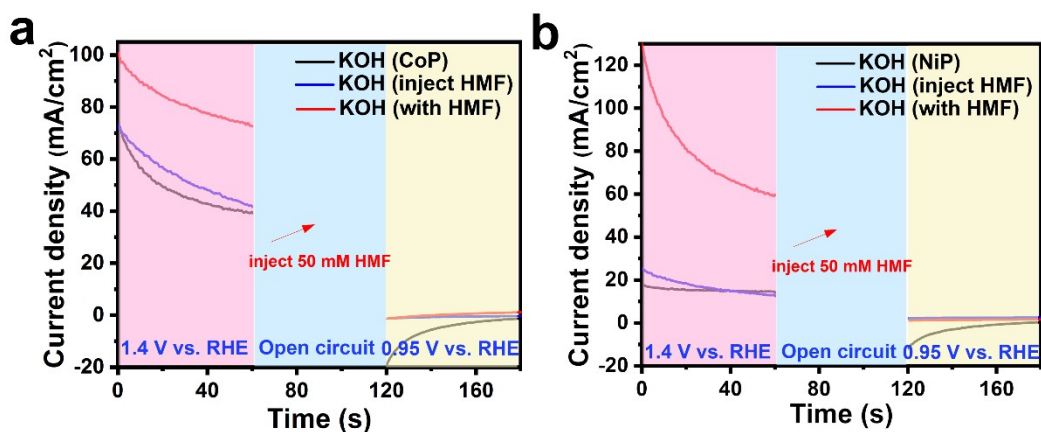
Fig. S10 Muti-potential step curves of the CoP and NiP.
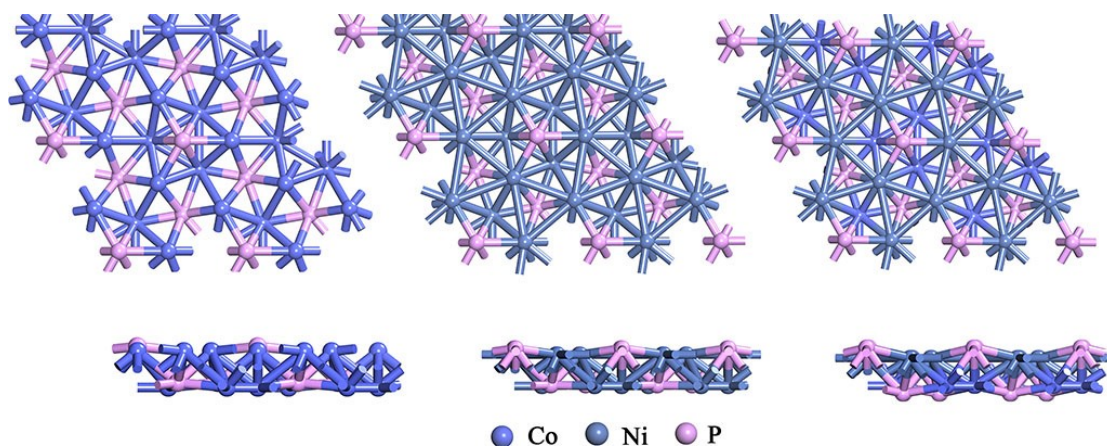
Co   Ni   P

Fig. S11 Calculation of the constructed models for CoNiP, CoP, and NiP.
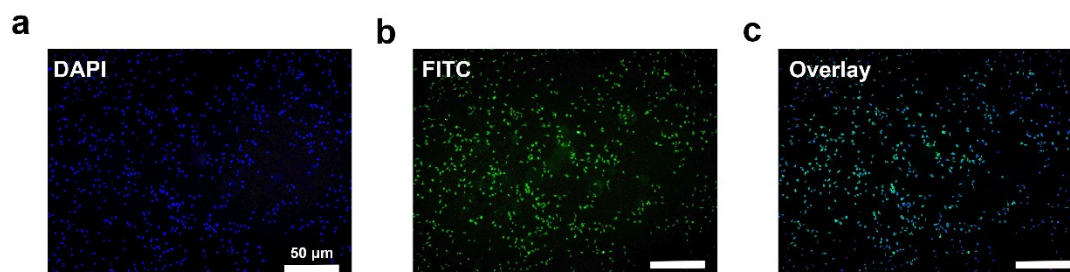
Fig. S12 CLSM images of HeLa cells incubated with DAPI and FITC-decorated CoNiP for 0.5 h.

Table S1. The relative energies (eV) for the H_2O doped at different sites of CoP, NiP and CoNiP.

Catalysis	S_{Co}	S_{Ni}	S_{Co-P}	S_{Ni-P}
CoP	-244.72	-	-244.72	-
NiP	-	-215.19	-	-215.19
CoNiP	-	-258.56	-	-258.04

1. K. B. John P. Perdew, * Matthias Ernzerhof, *Phys. Rev. Lett.*, 1996, **77**, 3865.
2. G. Kresse and J. Hafner, *Phys. Rev. B.*, 1993, **47**, 558-561.
3. G. Kresse and J. Hafner, *Phys. Rev. B.*, 1994, **49**, 14251-14269.

4. M. C. V. X. Wu, S. Nayak, V. Lotrich, G. Scoles, *J. Chem. Phys.* , 2001, **115**, 8748-8757.

5. S. Grimme, *J. Comput. Chem.*, 2006, **27**, 1787-1799.

6. P. E. Blöchl, *Phys. Rev. B.*, 1994, **50**, 17953-17979.

7. D. J. G. Kresse, *Phys. Rev. B.*, 1999, **59**, 1758.